

Closed-Loop Control of LiNbO₃ Quadrature Modulator for Coherent Communications

P. S. Cho, J. B. Khurgin*, and I. Shpantzer

CeLight, Inc., 12200 Tech Road, Suite 300, Silver Spring, MD 20904

*Johns Hopkins University, Dept. of ECE, Baltimore, MD 21218

Email: pscho@celight.com

Abstract: Closed-loop control of LiNbO₃ quadrature modulator for quaternary phase-shift-keyed transmission in coherent communications is reported. Simulations and experimental results of the feedback control loop for maintaining operating points of the quadrature modulator are described.

©2006 Optical Society of America

OCIS codes: (060.1660) Coherent communications; (060.5060) Phase modulation; (130.3120) Integrated optics devices

1. Introduction

Multi-level phase-shift-keying (PSK) offers high spectral efficiency transmission in coherent optical communication systems. Quaternary PSK (QPSK) format, in particular, has received much attention recently [1]. An optical QPSK signal can be generated, e.g., by an integrated LiNbO₃ quadrature modulator (QM) with two parallel Mach-Zehnder modulators (MZMs) nested in a MZ interferometer. Each MZM is driven to produce a binary PSK (BPSK) signal. An optical QPSK signal is produced when the two MZMs are biased at their null transmission points and the MZ interferometer is biased at the quadrature phase ($\pi/2$). An automatic feedback control loop that searches for these biases and phase operating points of the QM at initial startup and maintaining them during operation is essential. We report here a technique for such a closed-loop bias control for the QM using commercial off-the-shelf (COTS) components. Simulations and experimental results of the QM control loop for generation of 12.5 GSym/s QPSK signals are described.

2. QM control loop analysis and simulation

Fig. 1 shows a schematic of a QM with two push-pull type MZMs with RF and DC bias electrodes nested in a MZ interferometer with a phase electrode for quadrature bias. Consider a single MZM, the directly detected optical output power is: $P_o(t) = (kP_i/2)\{1 + \cos[\pi(V_s(t) + V_B)/V_\pi]\}$, where $V_s(t)$ is the NRZ drive signal with a peak-to-peak voltage swing V_{pp} , V_B is the bias voltage, V_π is the half-wave voltage, P_i is the input optical power, and k accounts for the insertion loss of the MZM. To generate optical BPSK signal, the MZM bias is set to the null transmission with $V_B = \pm V_\pi, \pm 3V_\pi, \dots$, and V_s varies between $\pm V_\pi$. The output average power over a period of time T is

$$\langle P_o(t) \rangle = \frac{kP_i}{2} \left(1 + \frac{1}{T} \int_0^T \cos \left[\frac{\pi}{V_\pi} (V_s(t) + V_B) \right] dt \right).$$

Taking the derivative of the above with respect to V_B and equating to zero gives

$$\frac{\partial \langle P_o(t) \rangle}{\partial V_B} = -\frac{kP_i}{2} \frac{\pi}{V_\pi} \frac{1}{T} \int_0^T \sin \left[\frac{\pi}{V_\pi} (V_s(t) + V_B) \right] dt = 0 \Rightarrow \sin \left[\frac{\pi}{V_\pi} (V_s(t) + V_B) \right] = 0.$$

The above is satisfied if $V_s = mV_\pi$ and $V_B = nV_\pi$ ($m, n = 0, \pm 1, \pm 2, \dots$). Taking the second derivative of $\langle P_o(t) \rangle$ with respect to V_B gives

$$\frac{\partial^2 \langle P_o(t) \rangle}{\partial V_B^2} = -\frac{kP_i}{2} \left(\frac{\pi}{V_\pi} \right)^2 \frac{1}{T} \int_0^T \cos \left[\frac{\pi}{V_\pi} (V_s(t) + V_B) \right] dt.$$

Therefore, the conditions for extrema of the average optical power are

$$\langle P_o(t) \rangle_{\max} \Rightarrow \frac{\partial^2 \langle P_o(t) \rangle}{\partial V_B^2} < 0 \Rightarrow \cos \left[\frac{\pi}{V_\pi} (V_s(t) + V_B) \right] > 0,$$

$$\langle P_o(t) \rangle_{\min} \Rightarrow \frac{\partial^2 \langle P_o(t) \rangle}{\partial V_B^2} > 0 \Rightarrow \cos \left[\frac{\pi}{V_\pi} (V_s(t) + V_B) \right] < 0.$$

For null transmission of the MZM, $V_B = \pm V_\pi, \pm 3V_\pi, \dots$, so that the above can be written as follows

$$\langle P_o(t) \rangle_{\max} \Rightarrow \frac{\partial^2 \langle P_o(t) \rangle}{\partial V_B^2} < 0 \Rightarrow \cos \left[\frac{\pi}{V_\pi} V_s(t) \right] < 0 \Rightarrow V_\pi < V_{pp} \leq 2V_\pi,$$

$$\langle P_o(t) \rangle_{\min} \Rightarrow \frac{\partial^2 \langle P_o(t) \rangle}{\partial V_B^2} > 0 \Rightarrow \cos \left[\frac{\pi}{V_\pi} V_s(t) \right] > 0 \Rightarrow 0 < V_{pp} < V_\pi.$$

Therefore, in order to maintain null transmission of the MZM for BPSK operation the average power of the MZM output should be maximized for $V_\pi < V_{pp} \leq 2V_\pi$ or minimized for $0 < V_{pp} < V_\pi$.

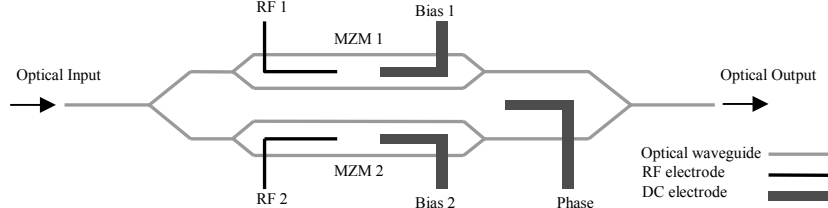


Fig. 1. Schematic of a quadrature modulator with two parallel MZMs nested in a MZ interferometer with a phase bias.

Fig. 2a shows a simulated output optical average power of the QM versus V_B for V_{pp} of $0.75V_\pi$ and $1.2V_\pi$. The simulation uses 12.5 Gb/s NRZ pseudo-random binary sequence (PRBS) signals with a word length of $2^{11}-1$ with realistic waveforms (finite rise and fall times and ringings) to drive the two MZMs of the QM biased to quadrature phase. The two NRZ signals are complementary with a 2-symbol relative time delay. Gaussian noise was added to the drive signal and to the input optical field to check the robustness of the response. As can be seen, the simulation result is consistent with the dependence of the average power on the MZM bias analyzed above.

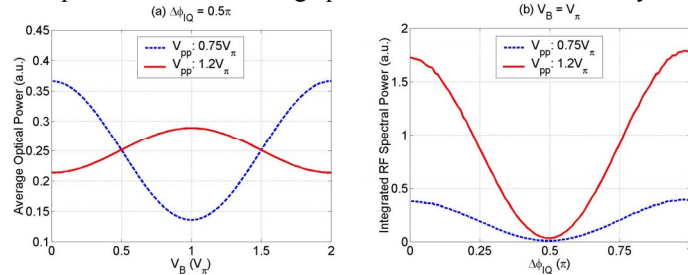


Fig. 2. Simulation results for (a) average power versus bias voltage of MZM and (b) integrated RF spectral power versus $\Delta\phi_{IQ}$ for NRZ drive signal swing of 0.75 and $1.2V_\pi$.

Consider now the phase bias of the MZ interferometer of the QM where the phase shift between the two BPSK signals (I and Q) is $\Delta\phi_{IQ}$. It can be shown that the directly detected output power of the QM is given by

$$P_{QM} = (kP_i/4) \left\{ 1 - \cos(\pi V_I/V_\pi)/2 - \cos(\pi V_Q/V_\pi)/2 + 2 \sin[\pi V_I/(2V_\pi)] \sin[\pi V_Q/(2V_\pi)] \cos(\Delta\phi_{IQ}) \right\},$$

where V_I and V_Q are the NRZ binary data signals applied to the two MZMs biased at their null transmission points ($V_B = V_\pi$). Assuming V_I and V_Q varies between $\pm V_\pi$ the detected output can thus be simplified as follows

$$P_{QM} = \begin{cases} kP_i [1 + \cos(\Delta\phi_{IQ})]/2, & \text{for } V_I = V_Q = \pm V_\pi, \\ kP_i [1 - \cos(\Delta\phi_{IQ})]/2, & \text{for } V_I = \pm V_\pi \text{ and } V_Q = \mp V_\pi. \end{cases}$$

It is clear that data-like binary pattern will appear at the output of the QM if the MZ interferometer is not in quadrature ($\Delta\phi_{IQ} \neq \pi/2$). The RF spectrum of P_{QM} contains low-frequency components due to this data pattern. Therefore, a minimum integrated RF spectral power of P_{QM} should be an indication that $\Delta\phi_{IQ}$ is close to $\pi/2$. Fig. 2b shows the simulated integrated RF spectral power of $P_{QM}(V_{RF})$ for V_{pp} of 0.75 and $1.2V_\pi$ versus $\Delta\phi_{IQ}$ using similar NRZ drive signals with Gaussian noise as in Fig. 2a. The results are in agreement with the analysis. Note that the dependence of V_{RF} on $\Delta\phi_{IQ}$ is not affected by V_{pp} . Based on the analysis and results shown in Fig. 2, a QM control loop algorithm and model was developed. The control loop uses a steepest decent algorithm to search for optimal operating points of the QM via dithering of its biases and phase. Fig. 3 shows typical simulation results of the control loop with Gaussian noise added to the drive signals and to the input optical field as before. One can see that the control loop is quite robust even in the presence of significant amount of amplitude and phase noise. Convergence to optimal operating points was observed for many random initial biases and phases of the QM tested.

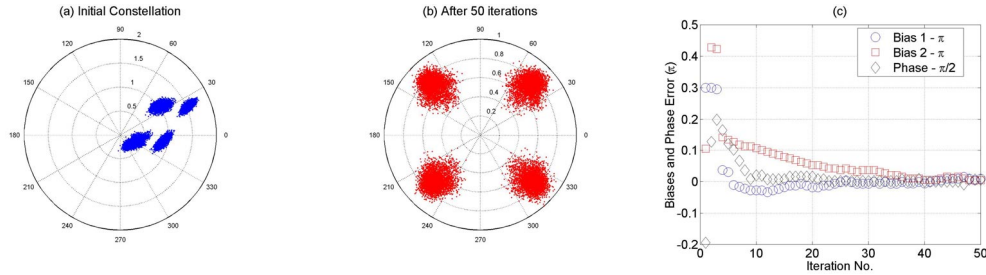


Fig. 3. Constellation plots of the QM optical output at startup (a) and after 50 iterations of the control loop (b). Plot of deviations of the two biases and phase from their optimal points (π and $\pi/2$) versus iteration number are shown in (c).

3. QM control loop experiment

An experiment on closed-loop control of the QM was conducted to investigate its performance for generation of a 12.5-GSym/s optical QPSK signal. A packaged LiNbO₃ QM was driven by two 12.5 Gb/s NRZ PRBS ($2^{15}-1$) signals. Details of the LiNbO₃ QM will be presented. The two NRZ signals are complementary with a 2-symbol relative time delay. The NRZ drive voltage swing applied to the QM was $V_{pp} \sim 1.2V_{\pi}$. The output of the QM was tapped off and directed to a 750-MHz photodetector where its output was divided into two with one path connected to a Schottky diode to extract the low-frequency RF spectral power (V_{RF}). The signal was amplified and directed to a COTS analog-to-digital converter (ADC) connected to a desktop computer (PC) running a code based on the control loop algorithm described earlier. The second path was amplified and directly connected to the ADC that provides monitoring of the optical average power by numerical averaging of the digitized signal. Outputs of a COTS digital-to-analog converter connected to the PC are directed to the two MZM bias ports and the phase port of the QM. This completes the QM feedback control loop.

The 12.5 GSym/s optical QPSK signal was directed to a receiver with an optical pre-amp and a band-pass filter. Differential detection of the 12.5 GSym/s QPSK signal was employed using a fiber-based asymmetric Mach-Zehnder (AMZ) interferometer [1] with a one-symbol differential delay (80 ps). The two outputs of the AMZ demodulator were directed to a 15-GHz balanced photoreceiver. Fig. 4 shows BER measurements of the differentially detected QPSK signal using the automatic control loop. Measurements using manual adjustment of the DC biases and phase of the QM by minimizing the BER are also shown. A power penalty of about 1 dB at 10^{-9} BER was observed for the control loop. This is attributed to the dithering and the relatively flat responses of V_{RF} and the average power near their optimal points as can be seen in Fig. 2. Nevertheless, the control loop concept was demonstrated and validated using COTS components. The QM control loop was operated continuously for about 20 hours with no degradation in performance. The control loop is expected to work for higher symbol rates since no high-speed components are required in the loop. The control loop also works for RZ format of the QPSK signal. Test results for generation and detection of 12.5 GSym/s RZ-DQPSK using the QM control loop will be discussed.

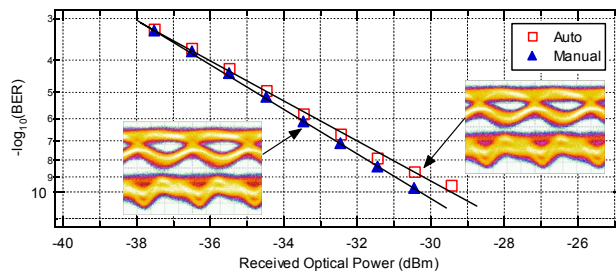


Fig. 4. BER versus received optical power of the differentially detected QPSK signal with automatic control loop or with manual adjustment of the QM. Insets show eye diagrams of the differentially detected 12.5 GSym/s QPSK signal (top) and waveforms of the directly detected output from the QM (bottom) for auto and manual control. Horizontal scale: 20 ps/div.

In summary, a closed-loop control for the QM using COTS components is reported. Simulations and experimental results on the control loop for generation of 12.5 GSym/s QPSK signals were described. The control loop shows a 1-dB sensitivity penalty compared with manual adjustment of the QM by minimizing the BER. Nevertheless, this is a relatively simple and inexpensive technique to maintain optimal operation of a QM for QPSK.

Reference

- [1] P. S. Cho, *et al.*, "Investigation of 2-bit/s/Hz 40-Gb/s DWDM transmission over 4×100-km SMF-28 fiber using RZ-DQPSK and polarization multiplexing," *Photon. Technol. Lett.*, **16**, 656-658 (2004).